



EXPERIMENTAL AND ANALYTICAL STUDY OF SEISMICALLY ISOLATED STRUCTURES WITH UPLIFT RESTRAINT

Panayiotis ROUSSIS¹ and Michael CONSTANTINOU²

SUMMARY

Experimental and analytical studies of a seismically isolated 5-story model structure are conducted to understand the behavior of a novel uplift-prevention Friction Pendulum isolator. Large-scale testing on the earthquake simulator at the University at Buffalo involves a number of simulated ground motions having a variety of frequency content and amplitude. A comprehensive analytical model is developed to predict the dynamic response of the model structure. The computer program 3D-BASIS-ME is enhanced to include an element representative of the mechanical behavior of the new isolator and used for comparison with experimental results. The experimental results generated demonstrate the effectiveness of the new isolator in uplift prevention and provide satisfactory evidence for the validity of the new element incorporated in 3D-BASIS-ME.

INTRODUCTION

With its appealing conceptual simplicity and its proven effectiveness, seismic isolation has become the epitome of seismic-resistant engineering in recent years. Having found a plethora of applications in many parts of the world over the past couple of decades, seismic isolation emerged as a pragmatic approach to providing earthquake resistance to structural systems.

The fundamental strategy underlying the seismic isolation technique involves decoupling the structure from the damaging horizontal ground motion, by means of additional flexibility and energy dissipation capability, thereby mitigating structural vibration and damage during seismic events.

Research developments in the areas of analytical modeling and experimental validation techniques have been paralleled by notable advances of seismic isolation device hardware. Introduced in this paper, is a novel uplift-prevention Friction Pendulum isolator, abbreviated hereafter as XY-FP. While a conventional Friction Pendulum in principle (Zayas [1], Mokha [2], Constantinou [3]), the proposed isolator is morphed into two perpendicular opposing concave beams forming a bi-directional (XY) motion mechanism. More

¹ Graduate Research Assistant, Department of Civil, Structural, and Environmental Engineering, State University of New York, Buffalo, NY 14260.

² Professor and Chairman, Department of Civil, Structural, and Environmental Engineering, State University of New York, Buffalo, NY 14260.

importantly, the configuration through which the two parts are interconnected permits tension to develop in the bearing, thereby preventing uplift.

The proposed isolation bearing has two unique properties: (1) effective uplift prevention; and (2) capability of providing different stiffness and energy absorption along the principal directions of the bearing. The latter property, can be exploited, for example, at expansion joints in bridges where different response in terms of displacement may be desired; neither a conventional FPS nor a rubber bearing can offer feasible displacement control in orthogonal directions. Additional benefits can be derived from the unique morphology of the new bearing. In particular, by encompassing much less structural material, the isolator at hand offers a lighter and more economical alternative. Moreover, it provides an architecturally flexible and elegant solution in terms of integration into a structural system for cases where space considerations are important, e.g., where the cylindrical shape of the conventional FP bearing becomes awkward or problematic under walls, as in the proximity of elevators and stairs.

This paper establishes the principles of operation and mathematical model of the newly introduced XY-FP isolator. The effectiveness of the XY-FP bearing in uplift prevention is demonstrated through testing of a large-scale steel-frame model structure on the earthquake simulator at University at Buffalo. Further, the computer program 3D-BASIS-ME (Tsopeles [4]) is enhanced to include an element representative of the mechanical behavior of the new isolator and used for comparison with experimental results. The experimental results generated attest to the validity and accuracy of analytical methods to predict the behavior of such systems.

DESCRIPTION AND MATHEMATICAL MODEL OF XY-FP ISOLATOR

While a conventional Friction Pendulum in principle, the proposed isolator consists of two opposing concave stainless steel beams forming a bi-directional (XY) motion mechanism (Figure 1). Under the imposed constraint to remain mutually perpendicular (except for small rotations about the vertical axis), the two beams can move independently relative to each other. In particular, the kinematics involved consists of two independent components: (1) sliding of upper beam along the (fixed) lower beam; and (2) sliding of upper beam with respect to the connecting block in direction perpendicular to the lower beam axis. In addition to geometric considerations, a distinguishing feature of the new isolator is its capability to prevent uplift. The configuration through which the two parts are interconnected permits tension to develop in the bearing, thereby preventing uplift.

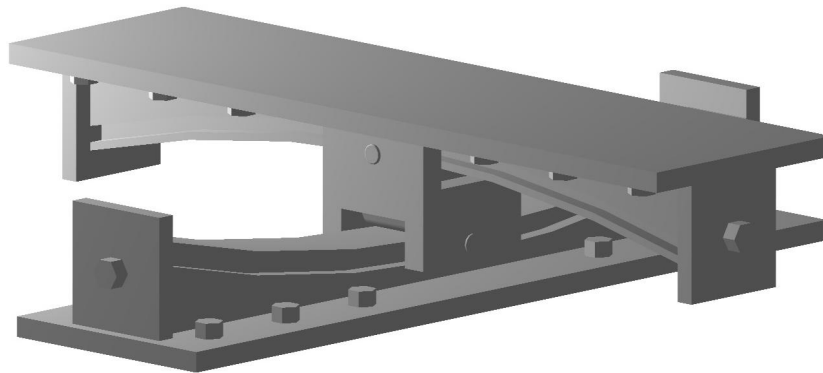


Figure 1: Three-dimensional view of the uplift-prevention XY-FP isolator

In formulating the mathematical model for the new XY-FP isolator, it is required that the force-displacement constitutive relationship be developed discretely for compressive and tensile bearing normal load. It is also important to note that the bi-directional motion admits decoupling along the principal axes of the bearing. Accordingly, the constitutive relationship can be conveniently stated with respect to the local axis system.

Figure 2 depicts a plan view of the bearing, whose orientation is defined by the angle θ the bottom beam makes with the global X-axis, in its deformed position $U = [U_x \ U_y]^T$ under the action of a lateral force $F = [F_x \ F_y]^T$. The corresponding displacement vector in the local axis system is given by

$$\begin{Bmatrix} U_1 \\ U_2 \end{Bmatrix} = \begin{bmatrix} \cos \theta & \sin \theta \\ -\sin \theta & \cos \theta \end{bmatrix} \begin{Bmatrix} U_x \\ U_y \end{Bmatrix} \quad (1)$$

The displacement components U_1 and U_2 are associated with independent motions along the bearing principal axes, namely sliding of upper beam along the lower beam (local axis 1), and sliding of upper beam in direction perpendicular to the lower beam (local axis 2). Figure 3 shows free body diagrams of the mobilized bearing segments under compressive and tensile bearing normal force.

The desired force-displacement relationship can be derived from equilibrium of forces in the horizontal (along axes 1 and 2) and vertical direction for each configuration of Figure 3. Assuming small displacements, the forces needed to induce displacement $U = [U_1 \ U_2]^T$ on the bearing in the local axis system are given collectively by

$$\begin{Bmatrix} F_1 \\ F_2 \end{Bmatrix} = N \begin{Bmatrix} U_1/R_1 \\ U_2/R_2 \end{Bmatrix} + |N| \begin{Bmatrix} \mu_1 \operatorname{sgn}(\dot{U}_1) \\ \mu_2 \operatorname{sgn}(\dot{U}_2) \end{Bmatrix}, \quad (2)$$

where R_1 and R_2 are the radii of curvature of the lower and upper concave beams, respectively; μ_1 and μ_2 are the associated sliding friction coefficients; N is the normal force on the bearing, positive when compressive; and $\operatorname{sgn}(\)$ is the signum function operating on the sliding velocities. It should be noted that, coefficients μ_1 and μ_2 can have different values depending on whether the bearing is in compression or tension.

In general, the normal force on the isolation bearing is a fast-varying function of time due to the vertical component of ground motion and the overturning moment effects. For a vertically rigid superstructure, the normal force on the bearing at any given time is synthesized by

$$N = W \left(1 + \frac{\ddot{u}_{gv}}{g} + \frac{N_{OM}}{W} \right), \quad (3)$$

where W is the weight acting on the isolator; \ddot{u}_{gv} is the vertical ground acceleration; and N_{OM} is the additional axial force due to overturning moment effects.

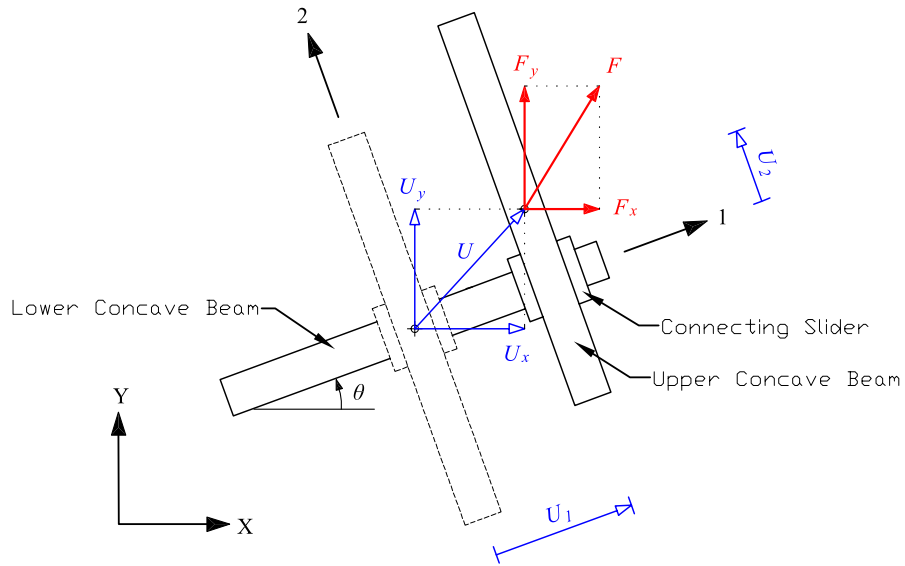


Figure 2: Plan view of XY-FP bearing in its deformed position

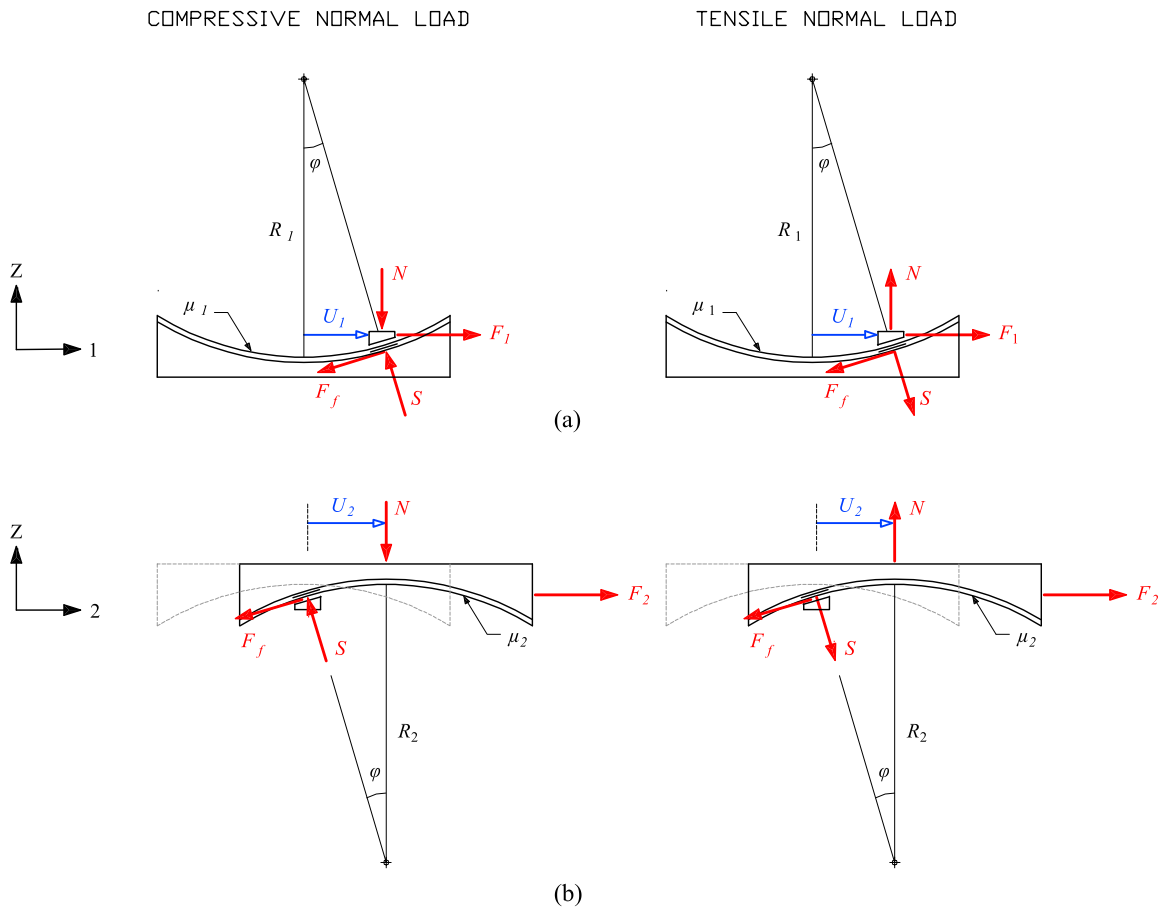


Figure 3: Free body diagrams of (a) connecting slider for motion along local axis 1, and (b) upper concave beam for motion along local axis 2, under compressive and tensile normal force

Evaluating the bearing normal force to this detail (Equation 3) is of utmost importance to the accuracy of the model. The fluctuation in the bearing axial force caused by the vertical component of ground motion and overturning moments can be large enough to cause reversal of the bearing axial force from compression to tension.

The coefficient of friction μ_i is a function of the sliding velocity \dot{U}_i and bearing normal force N . The velocity-dependency of the coefficient of friction, as proposed by Constantinou [5], is described by

$$\mu = f_{\max} - (f_{\max} - f_{\min})e^{-\alpha|\dot{v}|}, \quad (4)$$

where f_{\max} is the maximum friction coefficient at high velocity; f_{\min} is the minimum friction coefficient at zero velocity; and α is a parameter controlling the variation of friction with velocity.

Having defined the constitutive relation of the bearing with respect to the local axis system (Equation 2), the corresponding forces involved in the global axis system can be readily derived by

$$\begin{Bmatrix} F_x \\ F_y \end{Bmatrix} = \begin{bmatrix} \cos \theta & \sin \theta \\ -\sin \theta & \cos \theta \end{bmatrix}^T \begin{Bmatrix} F_1 \\ F_2 \end{Bmatrix} \quad (5)$$

EXPERIMENTAL PROGRAM

Model Description

The testing program on the earthquake simulator at the University at Buffalo involved a slender five-story model structure. It is the same frame used in previous testing of energy dissipation systems at the University at Buffalo (Chang [6]). A schematic and a photograph of the employed model are presented in Figure 4 and Figure 5, respectively. At a quarter length scale, the single-bay moment-resisting steel frame is square in plan with dimension of 1.321 m. The story heights are 1.092 m for the first story and 1.194 m for the other stories, for a total height of 5.868 m. The member layout is identical for all stories. The floors are comprised of MC6x12 (152.4x304.8) channel sections. In conforming to the similitude laws, artificial mass, in the form of steel plates and lead blocks, was added to the structure at all floor levels. The structure was attached to a rigid base under which the isolation system was installed. The distribution of mass is effectively 13.75 kN (3.1 kip) per floor and 37.8 kN (8.5 kip) for the base, for a total weight of 106.5 kN (24 kip).

It is worth noting that, due to the slenderness of the structure (height to width aspect ratio approximately 4.5), large overturning moment effects can potentially be induced on the structure under strong lateral base excitation. Indeed, the fluctuations in the bearing axial forces caused by overturning moments were large enough to cause reversal of the bearing axial force from compression to tension.

Installed beneath the rigid base, the isolation system consists of four new uplift-prevention Friction Pendulum isolators. The isolators used in this study were manufactured by Earthquake Protection Systems in Vallejo, California, with the dimensions shown in Figure 6. The isolator was constructed of stainless steel and was designed to have a displacement capacity of 203 mm (8 in). The radius of curvature of each concave beam was 990 mm (39 in).

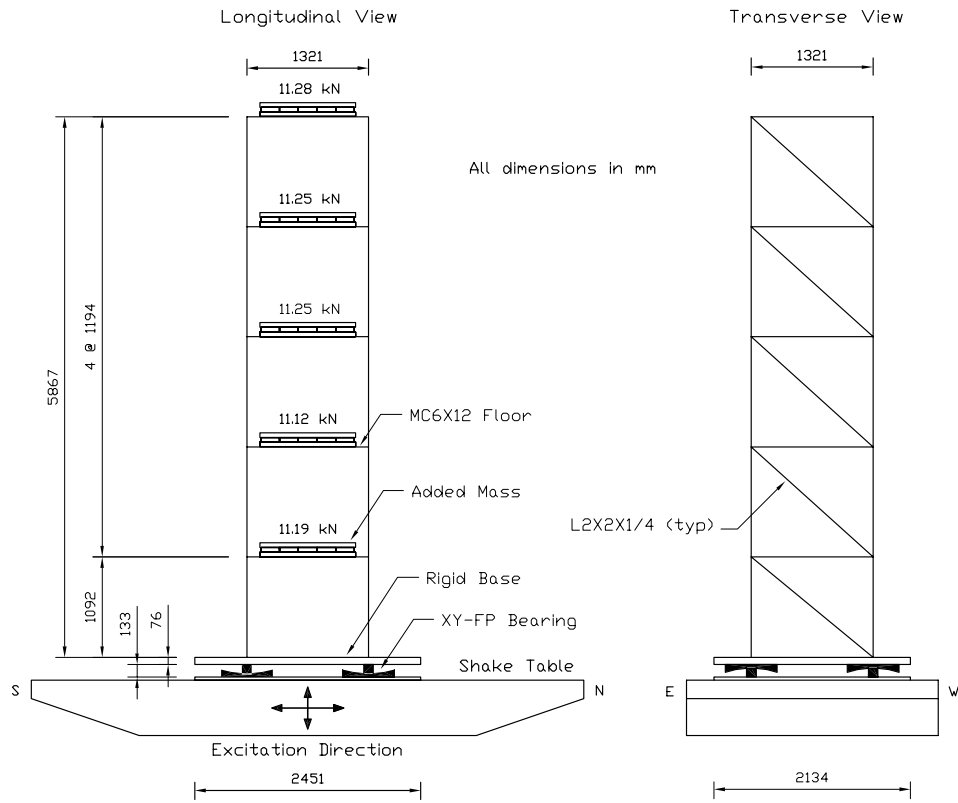
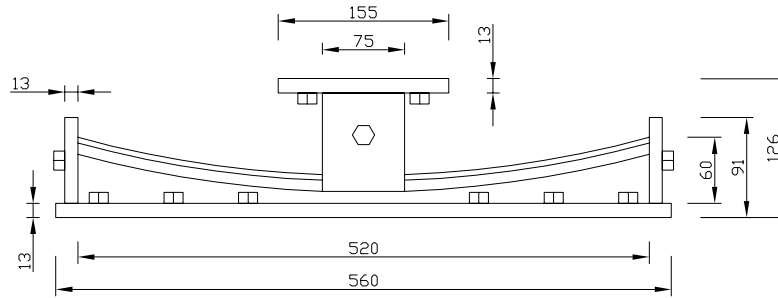


Figure 4: Schematic of tested 5-story isolated model structure



Figure 5: Photograph of tested five-story isolated model structure on seismic simulator of the University at Buffalo



All dimensions in mm

Figure 6: Two-dimensional view of the uplift-prevention XY-FP isolator used in this study

Testing Program

The large-scale testing on the earthquake simulator at the University at Buffalo utilized the slender five-story model structure described above. The testing program involved a number of actual horizontal and vertical ground motions having a variety of frequency content and amplitude. Table 1 lists the earthquake motions used in the testing along with their peak ground motion characteristics in prototype scale. Each record was compressed in time by a factor of two to conform to similitude requirements.

Table 1: List of earthquake motions and their characteristics in prototype scale

Notation	Excitation	Component	Peak Ground Motion		
			Disp. (mm)	Vel. (mm/s)	Accel. (g)
El Centro S00E	Imperial Valley, 1940	S00E	109	335	0.34
El Centro V	Imperial Valley, 1940	Vertical	92	107	0.21
Taft N21E	Kern County, 1952	N21E	67	157	0.16
Taft V	Kern County, 1952	Vertical	45	66	0.11
Newhall 90°	Northridge-Newhall, LA County Fire Station, 1994	90°	176	748	0.58
Newhall 360°	Northridge-Newhall, LA County Fire Station, 1994	360°	305	947	0.59
Newhall V	Northridge-Newhall, LA County Fire Station, 1994	Vertical	163	315	0.55
Sylmar 90°	Northridge-Sylmar, Parking Lot, 1994	90°	152	769	0.60
Sylmar V	Northridge-Sylmar, Parking Lot, 1994	Vertical	85	191	0.54
Kobe N-S	Kobe Station, Japan, 1995	N-S	207	914	0.83
Kobe V	Kobe Station, Japan, 1995	Vertical	103	383	0.34
Pacoima S74W	San Fernando, 1971 Pacoima Dam	S74W	108	568	1.08
Pacoima S16E	San Fernando, 1971 Pacoima Dam	S16E	365	1132	1.17
Pacoima V	San Fernando, 1971 Pacoima Dam	Vertical	182	565	0.71
Hachinohe N-S	Tokachi, Japan, 1968, Hachinohe	N-S	119	357	0.23

The instrumentation of the 5-story model structure consisted of accelerometers and displacement transducers which recorded respectively the horizontal accelerations and displacements of the frame at floor levels, the rigid base, and the shake table. In addition, the first-story columns were calibrated with strain gauge load cells to measure the first-story shear. To assess the accuracy of important recordings, measurements were contrasted with corresponding calculated quantities. For instance, to check the direct acceleration measurements, recorded floor absolute displacements were double-differentiated to obtain floor acceleration histories. In addition, the first-story shear was calculated by summing up floor inertia forces (product of floor mass and floor acceleration) and compared to the recorded first-story shear. Figure 7 depicts the instrumentation scheme employed in the testing program.

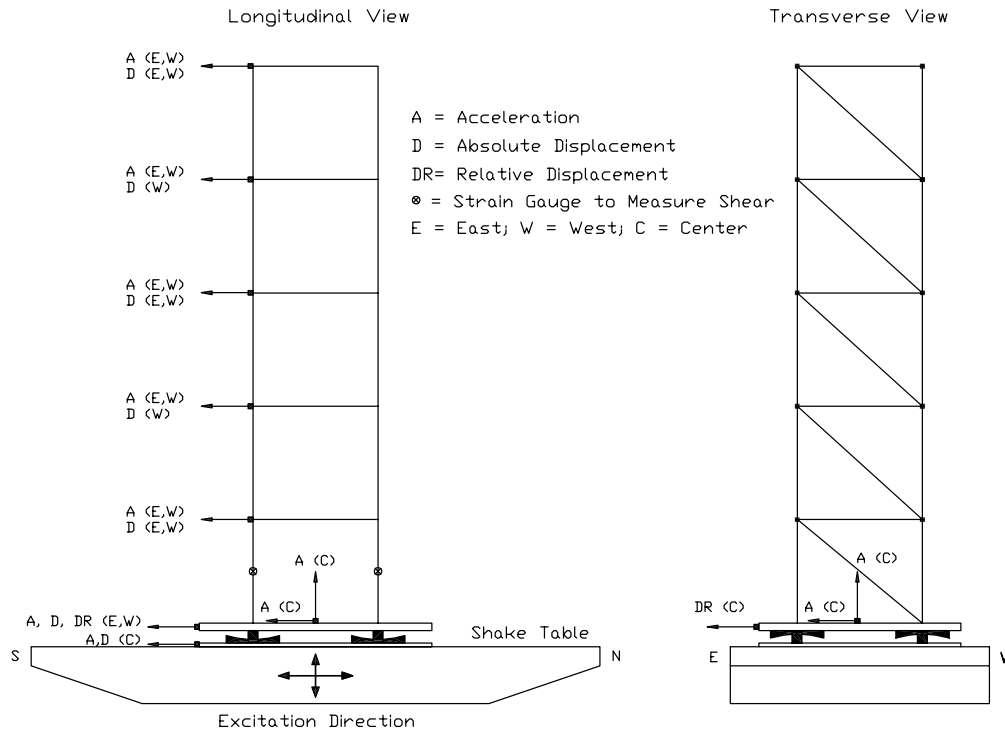


Figure 7: Instrumentation diagram for the 5-story test frame

The isolation system was rotated below the base plate for testing in different directions. Specifically, tests were done at 0-degree, 45-degree, and 90-degree angle of bottom bearing beam with respect to the excitation direction. A complete list of tests conducted is presented in Table 2.

Identification of Dynamic Characteristics of Model Structure

The testing program involved identification tests aimed at determining the dynamic characteristics of the non-isolated 5-story superstructure. The fixed-base condition was attained by locking the rigid base to the shake table via side plates, thereby preventing any relative motion. The tests were conducted using banded white noise excitation with acceleration amplitude of 0.05g and frequency content in the range of 0-40 Hz.

The desired mode shapes, frequencies, and damping ratios were determined using modal identification techniques (Reinhorn [7]). The method is based on the experimentally recorded floor acceleration histories and frequency response of the floor transfer functions. The transfer function is defined as an

Table 2: List of earthquake simulation tests conducted on the 5-story model structure

Excitation	Component	Intensity	Fixed Base	Isolated		
				Isolator Orientation		
				0°	90°	45°
El Centro	S00E	33%	√	-	-	-
		50%	-	√	-	-
100%		-	√	-	√	
200%		-	√	√	√	
	S00E + V	200%	-	√	√	√
Pacoima	S74W	100%	-	√	-	-
	S74W + V	100%	-	√	-	-
Pacoima	S16E	75%	-	√	-	-
		100%	-	√	√	√
		125%	-	-	√	√
		150%	-	-	√	-
	S16E + V	100%	-	√	√	√
Taft	N21E	50%	√	-	-	-
		100%	√	-	-	-
		400%	-	√	-	-
	N21E + V	400%	-	√	-	-
Hachinohe	N-S	100%	-	√	-	-
Sylmar	90°	100%	-	√	√	√
	90° + V	100%	-	√	√	√
Newhall	90°	100%	-	√	-	-
	90° + V	100%	-	√	-	-
Newhall	360°	100%	-	√	√	√
	360° + V	100%	-	√	√	√
Kobe	N-S	100%	-	√	-	-
	N-S + V	100%	-	√	-	-

output structural response normalized by a superimposed input base motion in the frequency domain. In particular, the transfer function for the j -th floor was obtained as the ratio of the Fourier transform of recorded horizontal acceleration of the j -th floor to the Fourier transform of the recorded base acceleration.

The dynamic characteristics of the fixed-base structure were also analytically determined using the program SAP2000 (Computers and Structures Inc. [8]). The first three mode shapes are graphically portrayed in Figure 8 and all extracted data pertinent to the superstructure identification (natural frequencies, damping ratios, and mode shapes) are listed in Table 3. The good agreement between experimentally derived and analytically calculated modal characteristics is evident.

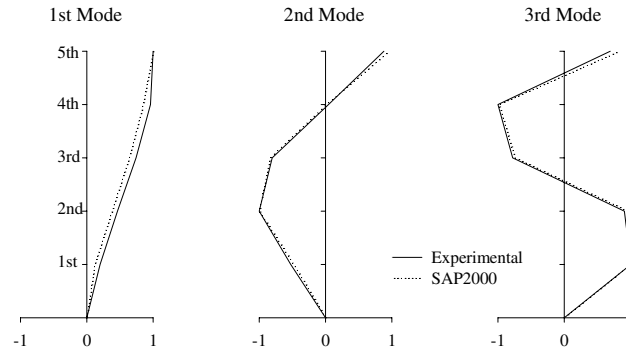


Figure 8: Schematic of influential mode shapes of fixed-base model structure

Table 3: Dynamic characteristics of fixed-base model structure

Mode	Method	Frequency (Hz)	Damping Ratio	Mode Shape				
				Floor 1	Floor 2	Floor 3	Floor 4	Floor 5
1	Experimental	2.3	0.061	0.200	0.460	0.740	0.960	1.000
	Analytical	2.4	-	0.120	0.380	0.640	0.850	1.000
2	Experimental	8.6	0.019	-0.526	-1.000	-0.807	0.044	0.877
	Analytical	8.2	-	-0.481	-1.000	-0.837	0.010	0.962
3	Experimental	16.4	0.011	1.000	0.903	-0.779	-1.000	0.690
	Analytical	16.4	-	1.000	0.958	-0.742	-0.983	0.833
4	Experimental	24.2	0.016	-1.000	0.333	0.637	-0.943	0.333
	Analytical	26.3	-	-1.000	0.272	0.653	-0.922	0.385
5	Experimental	29.7	0.018	0.810	-1.000	0.895	-0.551	0.223
	Analytical	34.6	-	0.914	-1.000	0.898	-0.578	0.178

ANALYTICAL PREDICTION OF RESPONSE

Analytical Model in 3D-BASIS

A comprehensive analytical model has been developed to predict the dynamic response of the seismically isolated model structure. The computer program 3D-BASIS-ME (Tsopelas [4]) has been enhanced to include an element representative of the mechanical behavior of the new isolator and used for comparison with experimental results.

Assumed to remain elastic at all times, the 5-story superstructure model in 3D-BASIS utilized a three-dimensional representation. Each floor mass is lumped into a single point mass having three degrees of freedom (two lateral and one torsional) in the horizontal plane. The dynamic characteristics required for the superstructure modeling were obtained from identification tests of the non-isolated frame.

The isolation system was modeled with spatial distribution and explicit nonlinear force-displacement characteristics of the individual isolation devices. To accommodate the mechanical behavior of the new XY-FP isolator, a new hysteretic element (TYPE8) was incorporated into the program. The new element is synthesized by two orthogonal uniaxial hysteretic elements allowing different frictional interface properties in the principal isolator directions. Contrary to the conventional FP isolator (TYPE6), the new element is capable of developing tension, and therefore providing uplift prevention. Moreover, different

frictional interface properties can be assumed under compressive and tensile isolator normal force.

The analysis accounted for: (a) the variability of axial load in isolators due to the vertical component of ground motion and overturning moment effects; (b) the dependency of friction on velocity; (c) different orientation of the isolator with respect to global X-direction; and (d) the initial non-zero displacement of the isolators (the permanent displacement from the immediate previous test).

Comparison of Analytical and Experimental Results

The validity of 3D-BASIS model, especially with reference to the newly introduced element representing the XY-FP isolator, was investigated by comparison of analytical predictions with experimental results. Figures 9-11 depict comparison between experimental and analytical results for horizontal and vertical

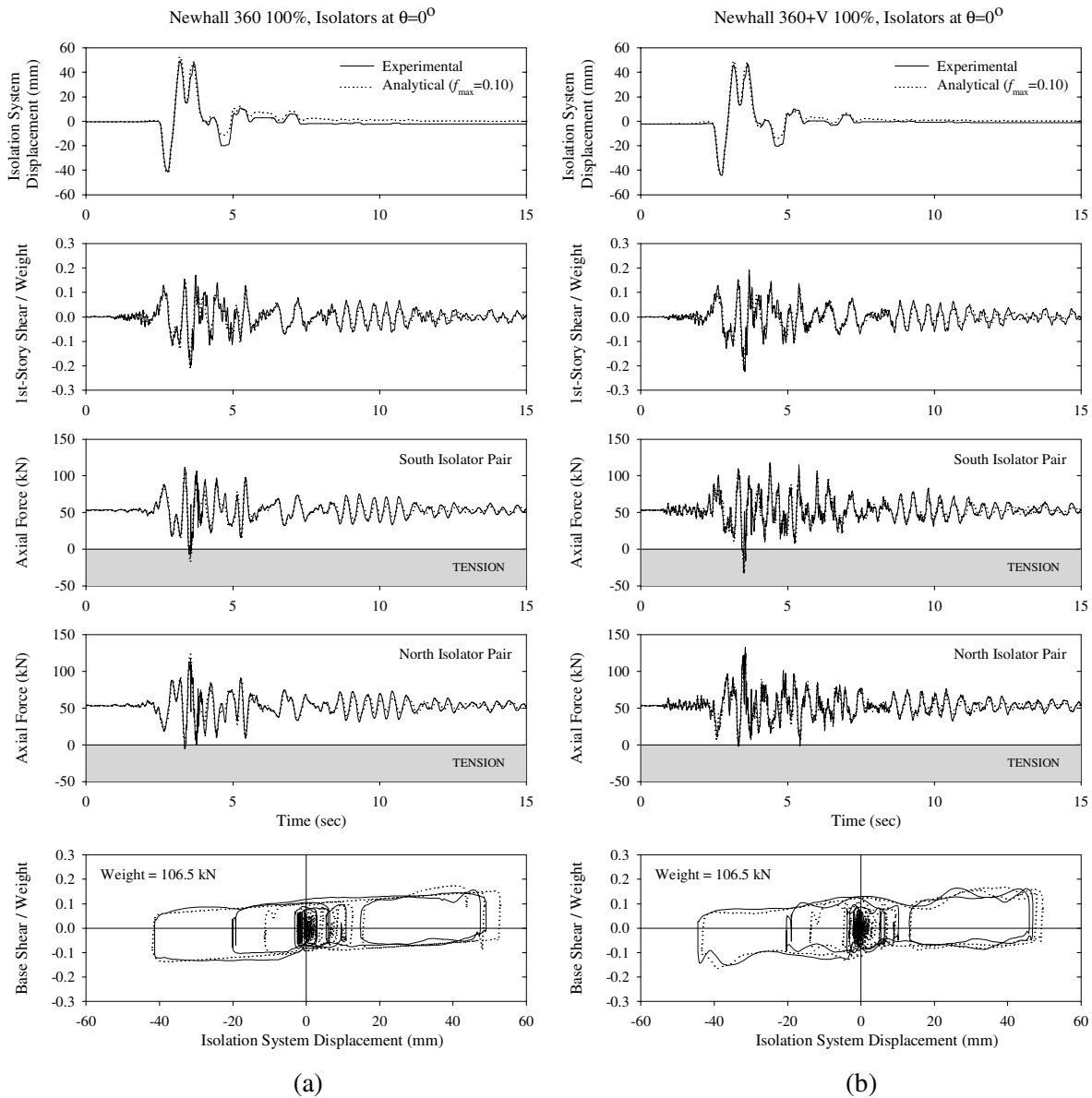


Figure 9: Comparison between experimental and analytical results for bearing orientation of 0°: (a) Newhall 360 100%; (b) Newhall 360+Vertical 100 %

input ground motions and for bearing orientation of 0, 90, and 45 degrees with respect to the global X-direction. The comparison was made in terms of histories of the isolation system displacement, the 1st-story shear, and the bearing axial force, as well as in terms of shear force-displacement loops for the isolation system.

Evidently, the analytical results are in very good agreement with the experimental results. Accordingly, the presented experimental results attest to the accuracy of the analytical model of the new isolator incorporated in 3D-BASIS-ME. This demonstrates that the behavior of XY-FP bearing is well understood to allow for accurate prediction of the response of isolated structures with these bearings.

Of particular interest is the axial force histories associated with the isolators, herein plotted per isolator

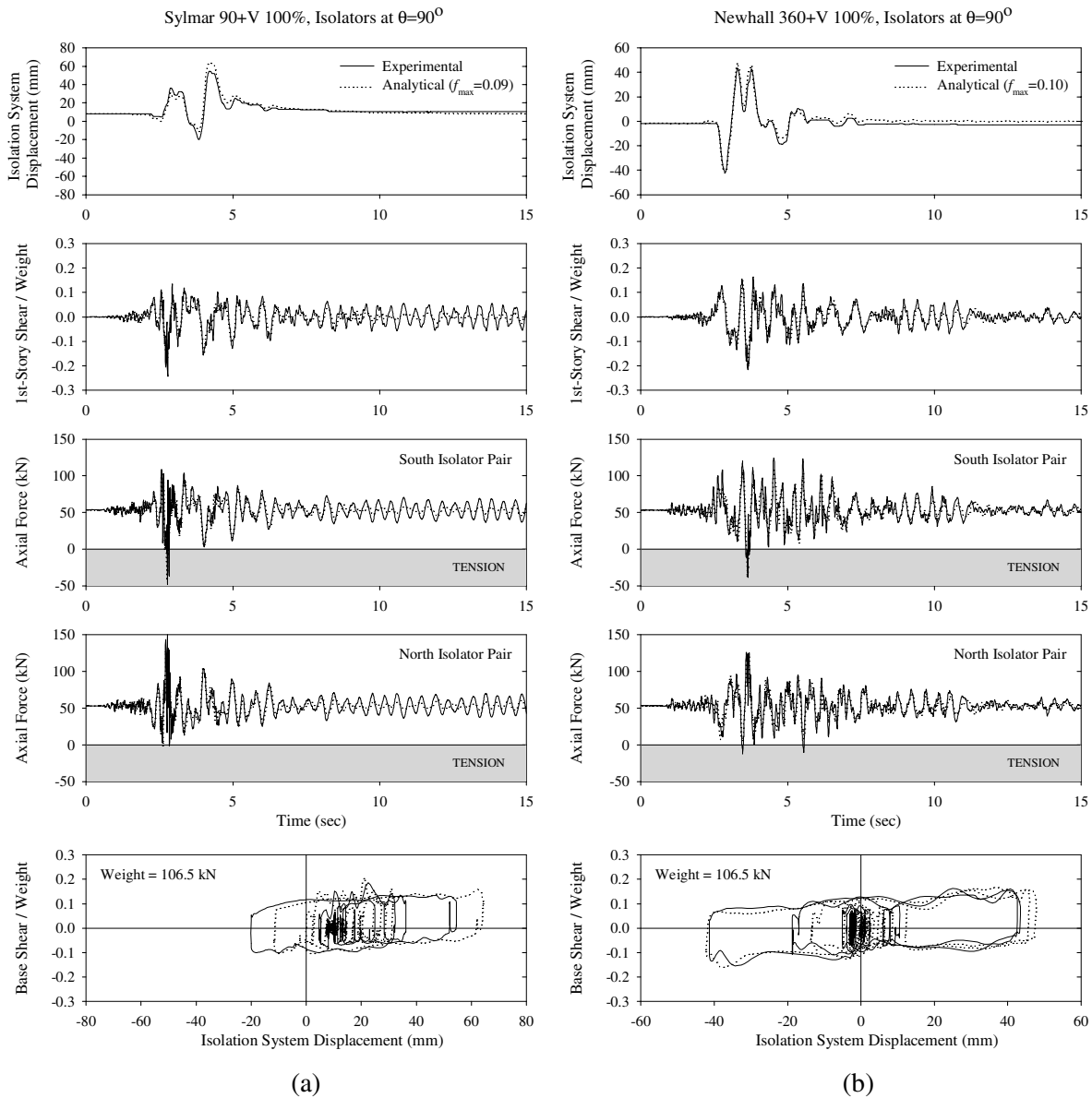


Figure 10: Comparison between experimental and analytical results for bearing orientation of 90°:
(a) Sylmar 90+Vertical 100%; (b) Newhall 360+Vertical 100%

pair. Due to the slenderness of the structure (height to width aspect ratio approximately 4.5), large overturning moment effects were induced on the bearings under strong lateral shaking. For most severe motions, the fluctuations in the vertical bearing loads caused by the overturning moments and the vertical component of ground motion were large enough to cause reversal of the bearing axial force from compression to tension (Figures 9-11). The experimental results generated demonstrate the effectiveness of the new XY-FP isolators in uplift prevention.

Figure 9 provides evidence of the effect of the vertical component of ground motion on the response of the isolated structure. In effect, the vertical ground acceleration modifies the axial load on the bearing (Equation 3), and therefore impacts both the restoring force and the friction force in the bearing constitutive relationship (Equation 2). This can be seen primarily in the wavy form of the isolation

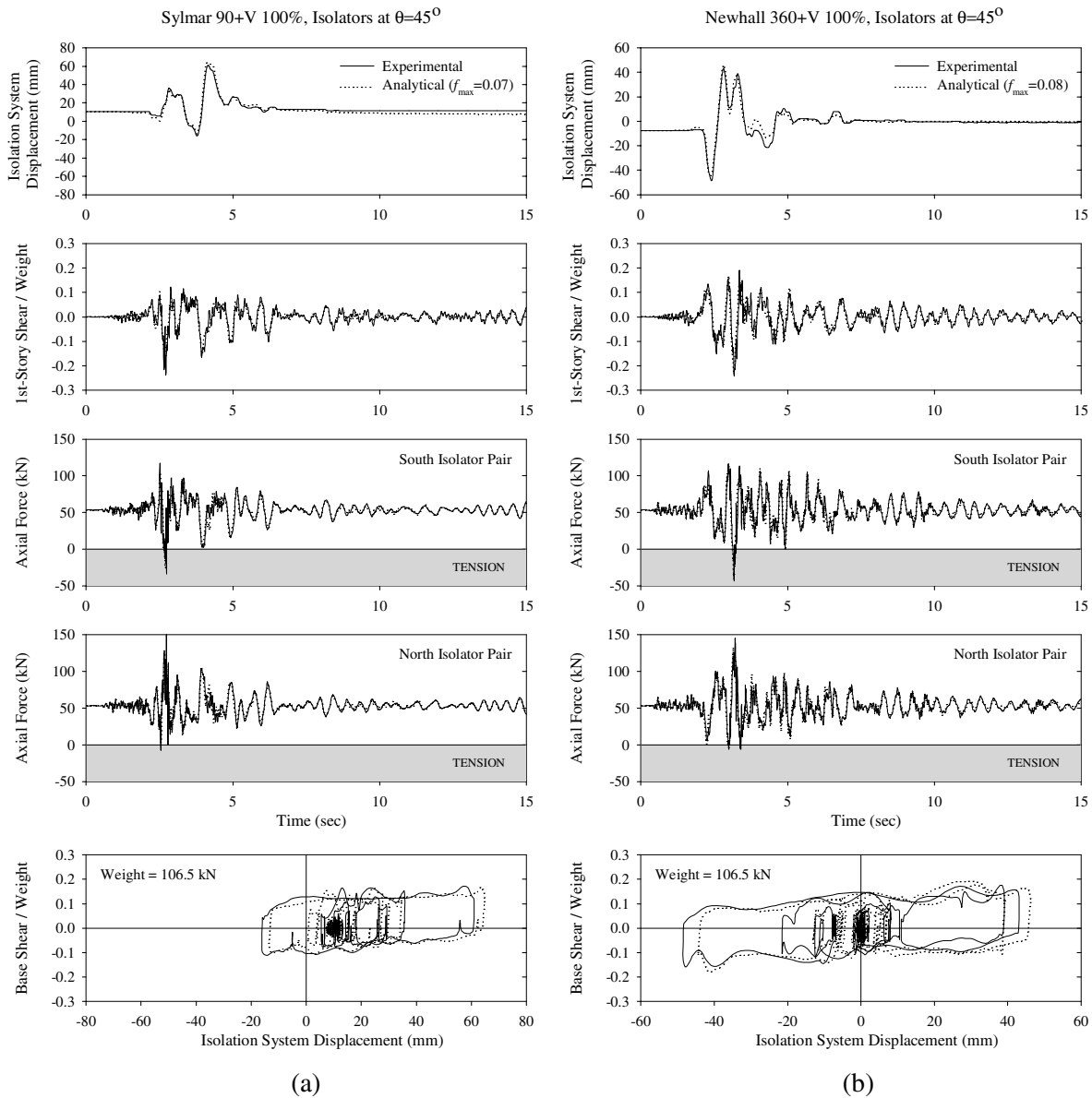


Figure 11: Comparison between experimental and analytical results for bearing orientation of 45°:
(a) Sylmar 90+Vertical 100%; (b) Newhall 360+Vertical 100%

system hysteresis loop and in the bearing axial force history. Figure 9(b) demonstrates that the amplification of the bearing axial force due to the vertical input may prove large enough to cause tension in the bearing.

CONCLUSIONS

Experimental and analytical studies of a seismically isolated building were conducted to understand the behavior of a novel uplift-prevention Friction Pendulum isolator. Large-scale testing on the earthquake simulator at the University at Buffalo utilized a 5-story model structure having a slender configuration. The testing program involved a number of actual ground motions with a variety of frequency content and amplitude.

A comprehensive analytical model was developed to predict the dynamic response of the model structure. The computer program 3D-BASIS-ME was modified to include an element representative of the mechanical behavior of the new XY-FP isolator and used for comparison with experimental results.

This investigation led to the following conclusions:

1. The experimental results generated demonstrate the effectiveness of the new XY-FP isolator in uplift prevention.
2. Satisfactory experimental evidence has been provided for the validity of the new XY-FP isolator model incorporated in 3D-BASIS-ME.
3. The response of the isolated structures subjected to severe earthquakes can be accurately predicted by analytical procedures.

ACKNOWLEDGEMENTS

This project was supported by the Multidisciplinary Center for Earthquake Engineering Research, which in turn was supported by the Earthquake Engineering Research Centers Program of the National Science Foundation, and Earthquake Protection Systems, Inc., Vallejo, CA.

REFERENCES

1. Zayas V, Low S, Mahin SA. "The FPS earthquake resisting system." Report UCB/EERC-87/01, Earthquake Engineering Research Center, University of California at Berkeley, 1987.
2. Mokha AS, Constantinou MC, Reinhorn AM. "Experimental study and analytical prediction of earthquake response of a sliding isolation system with spherical surface." Report NCEER-90-0020, National Center for Earthquake Engineering Research, State University of New York, Buffalo, New York, 1990.
3. Constantinou MC, Tsopelas PC, Kim Y-S, Okamoto S. "NCEER-TAISEI corporation research program on sliding seismic isolation systems for bridges: Experimental and analytical study of Friction Pendulum System (FPS)." Report NCEER-93-0020, National Center for Earthquake Engineering Research, State University of New York, Buffalo, New York, 1993.
4. Tsopelas PC, Constantinou MC, Reinhorn AM. "3D-BASIS-ME: Computer program for nonlinear dynamic analysis of seismically isolated single and multiple structures and liquid storage tanks." Report NCEER-94-0010, National Center for Earthquake Engineering Research, State University of New York, Buffalo, New York, 1994.
5. Constantinou MC, Mokha AS, Reinhorn AM. "Teflon Bearings in Base Isolation II: Modeling." Journal of Structural Engineering, ASCE, 116(2), 455-474, 1990.

6. Chang KC, Lai ML, Soong TT, Hao DS, Yeh YC. "Seismic behavior and design guidelines for steel frame structures with added viscoelastic dampers." Report NCEER-93-0009, National Center for Earthquake Engineering Research, State University of New York, Buffalo, New York, 1993.
7. Reinhorn AM, Soong TT, Lin RC, Yang YP, Fukao Y, Abe H, Nakai M. "1:4 scale model studies of active tendon systems and active mass dampers for aseismic Protection." Report NCEER-89-0026, National Center for Earthquake Engineering Research, State University of New York, Buffalo, New York, 1989.
8. Computers and Structures Inc. "SAP2000: Integrated Finite Element Analysis and Design of Structures." Version 7.5, Berkeley, CA, 1998.